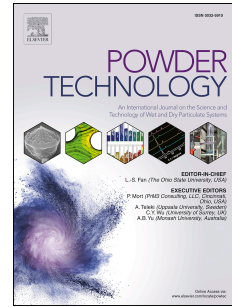


Journal Pre-proof

Numerical study of the solid flow behavior in a rotating drum based on a multiphase CFD model accounting for solid frictional viscosity and wall friction

Wenjie Rong, Yuqing Feng, Phil Schwarz, Peter Witt, Baokuan Li, Tao Song, Junwu Zhou



PII: S0032-5910(19)30830-7

DOI: <https://doi.org/10.1016/j.powtec.2019.10.034>

Reference: PTEC 14788

To appear in: *Powder Technology*

Received Date: 19 August 2019

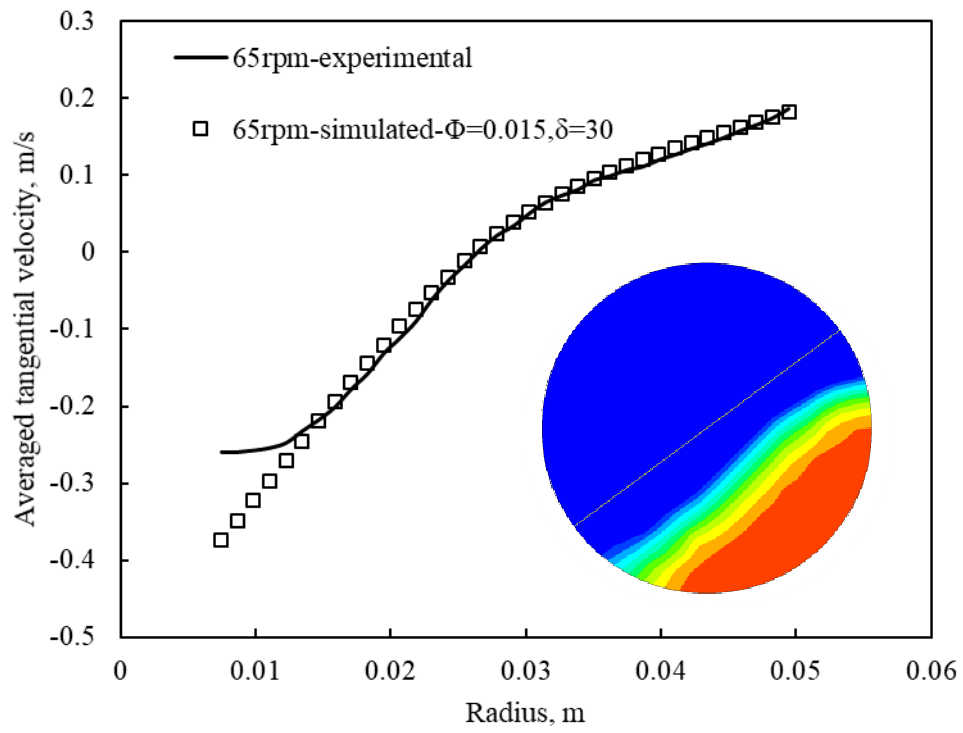
Revised Date: 24 September 2019

Accepted Date: 1 October 2019

Please cite this article as: W. Rong, Y. Feng, P. Schwarz, P. Witt, B. Li, T. Song, J. Zhou, Numerical study of the solid flow behavior in a rotating drum based on a multiphase CFD model accounting for solid frictional viscosity and wall friction, *Powder Technology* (2019), doi: <https://doi.org/10.1016/j.powtec.2019.10.034>.

This is a PDF file of an article that has undergone enhancements after acceptance, such as the addition of a cover page and metadata, and formatting for readability, but it is not yet the definitive version of record. This version will undergo additional copyediting, typesetting and review before it is published in its final form, but we are providing this version to give early visibility of the article. Please note that, during the production process, errors may be discovered which could affect the content, and all legal disclaimers that apply to the journal pertain.

© 2019 Published by Elsevier B.V.



Numerical Study of the Solid Flow Behavior in a Rotating Drum Based on a Multiphase CFD Model Accounting for Solid Frictional Viscosity and Wall Friction

Wenjie Rong^{a, b}, Yuqing Feng^{b, *}, Phil Schwarz^b, Peter Witt^b, Baokuan Li^{a, *}, Tao Song^c, Junwu Zhou^c

^a School of Metallurgy, Northeastern University, Shenyang 110819, China

^b CSIRO Mineral Resources Flagship, Clayton, VIC 3169, Australia

^c State Key Laboratory of Process Automation in Mining & Metallurgy, Beijing 100160, China

Corresponding authors: Yuqing Feng. Tel: +61 3 9545 8669 E-mail: yuqing.feng@csiro.au

Baokuan Li. Tel: +86 24 83672216 E-mail: libk@smm.neu.edu.cn

Abstract

In continuum-based models, the kinetic theory of granular flow (KTGF) provides a model for calculating solids stresses but has limitations in densely packed regions such as mills, kilns and rotating drums. The Eulerian-Eulerian multiphase model coupled with KTGF is evaluated in the present work. An additional frictional stress models were added, and their suitability evaluated. For the evaluation, a rotating drum at three rotational speeds (20 rpm, 42 rpm and 65 rpm) was analyzed. Compared with Positron Emission Particle Tracking (PEPT) measurement data from literature, Johnson and Jackson's model and Schaeffer's model for the frictional stress both showed a lower angle of repose regardless of the wall boundary condition used. Thus, a new frictional viscosity model based on granular pressure was proposed. By adjusting the specular coefficient of wall boundary condition, results of the present model agreed well with the PEPT measurements in terms of angle of repose and spatial velocity fields. In addition, considering that the actual Johnson and Jackson model for boundary condition includes two parts, collisional and frictional part, a discussion was made about boundary condition. The results showed that the validation of the proposed frictional viscosity model with experimental results could be completed at different rotational speeds by considering only the collisional part of the boundary condition with different specular coefficients or only the frictional part of the boundary condition with different angles of friction or both parts with the same specular

coefficient and angle of friction. Nevertheless, when the complete Johnson and Jackson model of boundary condition was applied, the same specular coefficient and angle of friction are used at different rotational speeds which is more physically meaningful. Moreover, it is found that the frictional contribution has greater influence on dynamic angle of repose than collisional contribution of the boundary condition in the current rotating drum.

Keywords: rotating drum; frictional viscosity; wall boundary condition; computational fluid dynamics (CFD); Eulerian-Eulerian model

1. Introduction

Rotating drums are widely used as rotary kilns, dryers, mixers, reactors and granulators in various industrial processes such as mineral, chemical, food and pharmaceutical process. The performance of rotating drum depends on a number of design and operating parameters and the flow regimes of the particles inside drums are classified as slipping, slumping, rolling, cascading, cataracting and centrifuging with increasing rotational speed of rotating drums [1, 2]. Due to the practicability and complexity, rotating drums have attracted numerous research studies, but the mechanism of solid flow behavior inside rotating drums is not completely understood.

Experimental and numerical methods have been applied to study solid flow behavior in rotating drums. Although several advanced experimental techniques, like Magnetic Resonance Imaging (MRI), Positron Emission Tomography (PET) and Positron Emission Particle Tracking (PEPT), can be used in the experiment, the sizes of drums and the scale of observation are limited [3-5]. Numerical methods provide an effective and cost-saving alternative way to study solid flow behavior in rotating drums. The two common numerical methods are Discrete Element Method (DEM) and Eulerian-Eulerian model. DEM resolves the solid motion and interaction at the particle-scale level which means the trajectory of each particle is calculated considering the forces acting on it [6]. The DEM provides detailed information about particles at the expense of high computational cost especially for large number of particles. Continuum Eulerian-Eulerian modelling based on the computational fluid dynamics (CFD) and the kinetic theory of granular flow is an alternative direction and it requires less computational cost in comparison and is preferred for large scale granular flow modelling [7].

In the Eulerian-Eulerian model, gas and particles are treated as interpenetrating continua and the granular flows are modeled as continuous fluid flows. The granular interactions are commonly modelled based on the kinetic theory of granular flow (KTGF). KTGF is a well-defined model but is limited to dilute systems that assume instantaneous binary collisions [8]. However, KTGF is found to be used in several papers to study dense flows in rotating drums [9-14]. Santos et al [9, 10] investigated hydrodynamic behavior in a rotating drum by experimental and numerical method. By using the kinetic model, the numerical results agreed well with the experimental observations. Based on Santos' work, Machado et al [12] also presented a numerical investigation using Eulerian-Eulerian model with KTGF of the particle dynamic flow in a rotary drum with one flight. It was observed that particle flow behavior was represented well in the flight at the rolling regime with appropriate specular coefficient and restitution coefficient. Moreover, Santos et al [11] and He et al [14] analyzed the segregation phenomenon in rotary drums using Eulerian-Eulerian model with KTGF. However, when the concentration of particles is high, instead of instantaneous collisions, the contact between the particles is long-lasting and the particles slide over each other [15]. Therefore, frictional viscosity was added to the solid viscosity in KTGF by other works [1-2, 15-19]. Delele et al [1] applied Schaeffer's model to consider the frictional viscosity in the multiphase CFD model. The accuracy of the model was checked based on the results of particle velocity, dynamic repose angle and active layer thickness, etc. Schaeffer's model was also applied in the work of Benedito et al [16]. They investigated the capability of CFD simulations in treating non-spherical particle dynamics in a rotating drum. The results showed that frictional viscosity was important for irregular particles modelling in a rotating drum. Similarly, in the work of Demagh et al [17], the calculation of frictional viscosity was based on Schaeffer's expression. But the Johnson and Jackson model was used for frictional pressure. This model was validated with experimental data. On the other hand, KTGF model with frictional viscosity cannot predict the dense granular flow patterns in rotating drums in the research studies of Huang et al [18, 19]. A dynamic angle of repose fitting method and a granular bed surface fitting method were proposed successively to approach the granular kinetic viscosity of the particles. Using the modified granular kinetic viscosity model, the predicted dynamic angle of repose was in good agreement with the experiment observation.

Based on the literature review, there is no consistency for the multiphase CFD model used for dense flow in rotating drums. Furthermore, modifications of KTGF-Eulerian approach can be done by developing new relations of the collisional-kinetic stress tensor and the frictional stress tensor in the constitutive Navier-Stokes equation [20].

When Eulerian-Eulerian model coupling with KTGF is used for modelling flows in rotating drums, implementation of appropriate boundary conditions is also critical to the prediction of flow pattern. It was demonstrated that wall friction significantly influence the flow performance [21]. In the literature, the commonly used wall boundary conditions for gas is no-slip, but for solids is no-slip, partial-slip or free-slip depending on the actual situation [1, 9-11]. The no-slip boundary condition is set by equating the tangential and normal velocities of the solid at wall to zero [12]. The partial-slip and free-slip boundary condition are implemented by Johnson and Jackson model which considers the tangential solids shear stress at a flat frictional wall. The shear stress on the boundary is the sum of collisional and frictional contributions [20]. Johnson and Jackson incorporated friction into the boundary condition in a heuristic way by considering a boundary at which some particles collide and the rest slide [22]. The momentum and energy transfer due to the colliding particles was characterized by a coefficient of specularity, and that of the sliding particles was determined by Coulomb friction. However, in most published research, only the collisional contribution was considered in rotating drums [12, 19, 23] or in other applications [24-32] by specifying a specularity coefficient. Since direct experimental measurement is not feasible for specularity coefficient, it was obtained by adjusting the value to fit some experimental data, which is very time-consuming, and the fit will have narrow applicability [33]. Thus, some researchers have considered that the specularity coefficient could be interpreted as a function of particle properties and interactions. Li et al [22] suggested an analytical expression for the specularity coefficient for a flat, frictional surface with a low frictional coefficient. The specularity coefficient was interpreted as a function of the particle-wall restitution coefficient, the frictional coefficient and the normalized slip velocity at the wall. Inspired by Li et al, Zhao et al [34] developed a model for specularity coefficient which was based on measurable particle properties and the data of Louge [35]. The model was tested for a granular Couette flow, a spouted bed and a circulating fluidized bed riser. The friction coefficient between particle and wall was found

to play a crucial role in the model.

Although the flow field is very sensitive to the choice of boundary condition, only a few attempts have taken frictional contribution into account. Haghgoo et al [36] examined the complete Johnson and Jackson model and another two models (Jenkins-Louge model and the model of Schneiderbauer et al) to assess their abilities to predict the dynamics of a dense gas-particle flow inside a three-dimensional bubbling bed. Their study demonstrated that the flows predicted by the three models of boundary condition were structurally similar. Li et al [22] mentioned frictional stress in the description of Johnson and Jackson model, but no detailed analysis was found in their work.

Generally, frictional stress comes into play only at high solids concentration, usually about 0.5 [22]. This is the reason why the frictional viscosity or frictional contribution in boundary condition were neglected in much open published research. However, in the current work, a prediction model was developed based on the available experimental measurements and DEM results, so it is easy to know that the volume fraction of solid is higher than 0.5 in most areas in rotating drums [5, 36-37]. As a result, Eulerian-Eulerian model coupled with KTGF was used to study the dense flow in the rotating drum with the consideration of frictional viscosity and frictional contribution in boundary condition. Firstly, Schaeffer's model and Johnson and Jackson model of the granular frictional viscosity were tested with only collisional boundary condition being considered. Then a frictional viscosity model based on granular pressure was proposed. By using the proposed model with the same boundary condition, the numerical results agreed well with experiment results. Finally, the Johnson and Jackson model for boundary condition was further analyzed. A comparison was made between collisional and frictional contributions to the boundary condition.

2. Material and methods

The Eulerian-Eulerian model considers the gas and solid as continuous and fully interpenetrating. Both phases are described by a set of fundamental and constitutive equations solved in a Eulerian frame of reference.

2.1 Conservation mass and momentum equations and drag model

The continuity equations for gas phase and solid phase are as follows:

$$\frac{\partial}{\partial t}(\alpha_g \rho_g) + \nabla \cdot (\alpha_g \rho_g \vec{v}_g) = 0 \quad (1)$$

$$\frac{\partial}{\partial t}(\alpha_s \rho_s) + \nabla \cdot (\alpha_s \rho_s \vec{v}_s) = 0 \quad (2)$$

where α is the volume fraction, ρ is the density, kg/m^3 and \vec{v} is the velocity vector, m/s . The subscripts s and g represent solid phase and gas phase, respectively. The volume fractions of the gas and solid phases satisfy the following relationship:

$$\alpha_s + \alpha_g = 1 \quad (3)$$

The equations of momentum balance for gas phase and solid phase are given by:

$$\frac{\partial}{\partial t}(\alpha_g \rho_g \vec{v}_g) + \nabla \cdot (\alpha_g \rho_g \vec{v}_g \vec{v}_g) = -\alpha_g \nabla p + \nabla \cdot \bar{\tau}_g + \alpha_g \rho_g \vec{g} + K_{sg}(\vec{v}_s - \vec{v}_g) \quad (4)$$

$$\frac{\partial}{\partial t}(\alpha_s \rho_s \vec{v}_s) + \nabla \cdot (\alpha_s \rho_s \vec{v}_s \vec{v}_s) = -\alpha_s \nabla p - \nabla p_s + \nabla \cdot \bar{\tau}_s + \alpha_s \rho_s \vec{g} + K_{sg}(\vec{v}_g - \vec{v}_s) \quad (5)$$

where p , g , and p_s are the pressure (Pa) shared by all phases, gravity acceleration (m/s^2) and solid pressure (Pa), respectively. K_{sg} is the interphase momentum exchange coefficient and the last terms in Eqs. (4) and (5) are the momentum exchanged between gas and solid phase. In this work, only drag force is considered and it is determined based on the model developed by Gidaspow which a combination of the Wen and Yu model and the Ergun equation [17]. $\bar{\tau}$ is the stress-strain tensor. In the Newtonian form, $\bar{\tau}_g$ and $\bar{\tau}_s$ are written as:

$$\bar{\tau}_g = \mu_g \left[\nabla \vec{v}_g + \nabla \vec{v}_g^T \right] - \frac{2}{3} \mu_g (\nabla \cdot \vec{v}_g) \bar{I} \quad (6)$$

$$\bar{\tau}_s = \alpha_s \mu_s \left[\nabla \vec{v}_s + \nabla \vec{v}_s^T \right] + \alpha_s \left(\lambda_s - \frac{2}{3} \mu_s \right) \nabla \cdot \vec{v}_s \bar{I} \quad (7)$$

where \bar{I} , μ and λ are the unit tensor, viscosity ($\text{kgm}^{-1}\text{s}^{-1}$) and bulk viscosity ($\text{kgm}^{-1}\text{s}^{-1}$), respectively.

The solid pressure, viscosity and bulk viscosity can be obtained from KTGF, as discussed below.

2.2 Kinetic theory of granular flow

The solids stress tensor contains shear and bulk viscosities arising from particle momentum exchange due to translation and collision. A frictional component of viscosity can also be included to account for the viscous-plastic transition that occurs when the volume fraction of solid phase reaches the packing limit. The collisional and kinetic parts, and the optional frictional part are added to give the solids shear viscosity [38]:

$$\mu_s = \mu_{s,col} + \mu_{s,kin} + \mu_{s,fr} \quad (8)$$

The collisional part of the shear viscosity is modeled as [39]:

$$\mu_{s,col} = \frac{4}{5} \alpha_s \rho_s d_s g_0 (1 + e_s) \left(\frac{\Theta_s}{\pi} \right)^{\frac{1}{2}} \quad (9)$$

The expression of kinetic viscosity is from Gidaspow et al. [39]:

$$\mu_{s,kin} = \frac{10 \rho_s d_s \sqrt{\Theta_s \pi}}{96 g_0 (1 + e_s)} \left[1 + \frac{4}{5} \alpha_s g_0 (1 + e_s) \right]^2 \quad (10)$$

The solid bulk viscosity, which represents the resistance to compression of the solid phase, is calculated by [40]:

$$\lambda_s = \frac{4}{3} \alpha_s^2 \rho_s d_s g_0 (1 + e_s) \left(\frac{\Theta_s}{\pi} \right)^{\frac{1}{2}} \quad (11)$$

where d_s is the particle diameter (m), g_0 is the radial distribution function at contact, e_s is the coefficient of restitution for particle collisions and Θ_s is the granular temperature (m^2/s^2). The granular temperature is proportional to the kinetic energy of the fluctuating particle motion:

$$\Theta_s = \frac{1}{3} u_s u_s \quad (12)$$

where u_s is the fluctuating solids velocity in the Cartesian coordinate system (m/s).

The transport equation of the granular temperature derived from kinetic theory takes the form [41]:

$$\frac{3}{2} \left[\frac{\partial}{\partial t} (\alpha_s \rho_s \Theta_s) + \nabla \cdot (\alpha_s \rho_s \vec{v}_s \Theta_s) \right] = (-p_s \bar{l} + \bar{t}_s) : \nabla \vec{v}_s + \nabla \cdot (k_{\Theta_s} \nabla \Theta_s) - \gamma_{\Theta_s} + \varphi_{gs} \quad (13)$$

where k_{Θ_s} , γ_{Θ_s} and φ_{gs} are the diffusion coefficient, the collisional dissipation of energy and the energy exchange between the gas and solid phase, respectively. Three terms are given in the following [39, 42]:

$$k_{\Theta_s} = \frac{150 \rho_s d_s \sqrt{\Theta_s \pi}}{384 g_0 (1 + e_s)} \left[1 + \frac{64}{5} \alpha_s g_0 (1 + e_s) \right]^2 + 2 \alpha_s^2 \rho_s d_s g_0 (1 + e_s) \left(\frac{\Theta_s}{\pi} \right)^{\frac{1}{2}} \quad (14)$$

$$\gamma_{\Theta_s} = 3(1 - e_s^2) \alpha_s^2 \rho_s g_0 \Theta_s \left(\frac{4}{d_s} \sqrt{\frac{\Theta_s}{\pi}} - \nabla \cdot \vec{v}_s \right) \quad (15)$$

$$\varphi_{gs} = -3 K_{sg} \Theta_s \quad (16)$$

The solid pressure represents the normal forces caused by collisions between particles:

$$p_s = \alpha_s \rho_s \Theta_s + 2 \alpha_s^2 \rho_s g_0 \Theta_s (1 + e_s) \quad (17)$$

The radial distribution function at contact, g_0 , is a correction factor that modifies the probability of

collisions between particles when the solid granular phase becomes dense. In the current paper, g_0 is calculated by [43]:

$$g_0 = \frac{1}{1 - \left(\frac{\alpha_s}{\alpha_{s,max}}\right)^{1/3}} \quad (18)$$

where $\alpha_{s,max}$ is the packing limit.

2.3 Frictional stress model

A commonly used model of frictional viscosity in dense flow is determined by Schaeffer [43]:

$$\mu_{s,fr} = \frac{p_s \sin \beta}{2\sqrt{I_{2D}}} \quad (19)$$

where β is the angle of internal friction. I_{2D} is the second invariant of the deviator of the strain rate tensor [15].

In dense flow where the secondary volume fraction for a solid phase nears the packing limit, the generation of stress is mainly due to friction between particles. The frictional stress is usually written in Newtonian form [44]:

$$\tau_{s,fr} = -p_{s,fr} \bar{\mathbf{I}} + \mu_{s,fr} (\nabla \vec{v}_s + \nabla \vec{v}_s^T) \quad (20)$$

where $p_{s,fr}$ is the frictional stress, Pa.

The frictional stress is added to the stress predicted by the kinetic theory when the solids volume fraction exceeds a critical value, $\alpha_s > \alpha_{s,min}$.

$$p_s = p_{s,kin} + p_{s,fr} \quad (21)$$

$$\mu_s = \mu_{s,kin} + \mu_{s,fr} \quad (22)$$

A semi-empirical equation was proposed by Johnson and Jackson for the frictional stress [20]:

$$p_{s,fr} = Fr \frac{(\alpha_s - \alpha_{s,min})^n}{(\alpha_{s,max} - \alpha_s)^p} \quad (23)$$

where Fr , n and p are empirical material constants. $\alpha_{s,min}$ is the critical value. Different critical value was used in papers [9] and some authors did not mention about the magnitude of the critical value when they applied the concept [14, 17-18]. In the current paper, $\alpha_{s,min}$ is set 0.5.

The frictional viscosity is then related to the frictional stress by the linear law proposed by Coulomb [45]:

$$\mu_{s,fr} = \frac{p_{s,fr} \sin \beta}{2\sqrt{I_{2D}}} \quad (24)$$

It was found that Schaeffer's model and Johnson and Jackson's model cannot satisfactorily predict the dense flow in the current rotating drum. In dense flow at low shear, where the secondary volume fraction for a solid phase nears the packing limit, the generation of stress is mainly due to friction between particles. From Eq. (18), it can be seen that the radial distribution function tends to infinity as the volume fraction tends to the packing limit. Granular pressure calculated based on Eq. (17) has similar trend. Thus, it would then be possible to use the granular pressure directly in the calculation of the frictional viscosity [38]. Accordingly, a new frictional viscosity model was proposed:

$$\mu_{s,fr} = k \cdot p_s \quad (25)$$

where k is coefficient with unit of s in the current work and the value of k will be discussed in Chapter 3.1.

2.3 Boundary conditions and numerical solution

There are two methods that can be used in Fluent for inputting drum movement, mesh motion and moving wall. In the present work, mesh motion is used because it is not possible to set specular coefficient from the boundary condition due to numerical inconsistency (two different speed values at the same cell) when using moving wall [16].

The Johnson and Jackson model for wall boundary condition is as follows [20, 47-48]:

$$\vec{\tau}_s = -\frac{\pi}{6}\sqrt{3}\varphi \frac{\alpha_s}{\alpha_{s,max}} \rho_s g_0 \sqrt{\Theta_s} \vec{U}_{sw} - N_f \tan \delta \quad (26)$$

where φ is the specular coefficient. \vec{U}_{sw} is the relative velocity between the wall and particles in contact with it, m/s. N_f is normal frictional component of stress, Pa. δ is angle of friction between the wall and the particulate material, °. The first and second terms in the right side of Eq. (26) represent the stress acting on the boundary due to particle-wall collision and friction, respectively [47]. As mentioned before, in most published research, only the first term was taken into account. One of the reasons could be that the specular coefficient is easily to set in the boundary condition using Fluent. So, at the beginning of this work, the specular coefficient has been adjusted for different rotational speeds to fit experimental data like other work did. Then, the collisional part of the boundary

condition was reproduced by using udf (user-defined function) code in the form of shear stress. Once the reproduction was achieved, the frictional part was not difficult to add in the boundary condition equation in the code. Based on this method, the complete Johnson and Jackson boundary condition was applied and analyzed.

Simulation conditions for the rotating drum were based on the experimental configuration in Parker's work [5]. A horizontal rotating drum with diameter of 100 mm was simulated. The drum was approximately 35 % filled by mono-sized glass spheres with diameter of 3 mm. The drum rotates around its axis at a rotation speed from 20 to 65 rpm. The detailed parameters are depicted in **Table 1**. Restitution coefficient of particle is specified as 0.9 considering that experimental measurement is hard to implement and 0.9 is commonly used in similar researches [9, 12, 15, 17-19]. The simulations were carried out in a 2D rotating drum using the CFD code (Fluent 19.0). The mesh size was 5 mm after conducting a mesh sensitivity study as seen in Fig. 1. The initial volume fraction of solid was 0.6 and the packing limit was 0.63. The SIMPLE algorithm was used for pressure-velocity coupling and the equations were discretized using a second order upwind scheme. A fixed time-step of 0.001s was used and the convergence criterion between two interactions was set to 1×10^{-3} . To get the average results, 6 revolutions have been done for the rotating drum and the corresponding calculation times are 6s, 8.6s and 18s for 20 rpm, 42 rpm and 65 rpm, respectively.

3. Results and discussion

3.1 Test configuration

In this paper, frictional viscosity and wall boundary condition were two main aspects considered in the numerical model. As mentioned above in Chapter 2.3, three models of granular frictional viscosity were involved, and two parts of the boundary condition were analyzed at different rotational speeds. All the model configurations are summarized in **Table 2**. Firstly, different models of granular frictional viscosity were compared using the same boundary condition which means only collisional part was considered. The corresponding cases are case 01 to case 05. When the proposed model of frictional viscosity was used, the k in Eq. (25) was determined by a trial-and-error method. From the experimental results, it can be found that most particles in the rotating drum were in contact with each other, so frictional viscosity of solid phase should always exist. Inspired by the Johnson and Jackson

model of frictional stress, k was divided into two parts with solid volume fraction of 0.6 as the boundary. A relatively smaller value was guessed for the volume fraction of solid phase lower than 0.6 and a higher value was guessed for denser part. This trial-and-error procedure was repeated until the predicted numerical results agreed well with experimental observation in terms of dynamic angle of repose and spatial velocity fields. The k used in the current work was 0.35 s, 0.4 s and 0.5 s for volume fraction of the solid phase lower than 0.6 at the rotational speeds of 20 rpm, 42 rpm and 65 rpm respectively, and 0.2 s for volume fraction of the solid phase higher than 0.6 at all rotational speeds simulated.

Then, the Johnson and Jackson model for boundary condition was deeply analyzed by adjusting the specular coefficient and the angle of friction which corresponds to cases 05 to 09. In order to ensure comparability, the values of k used in cases 06 to 09 were the same as that used in case 05. In the actual simulation process, the specular coefficient ranged from 0.01 to 1. But for simplification, only representative values are shown in **Table 2**. The angle of friction assumed when considering the frictional contribution in boundary condition was based on the measurement data of similar particles in the work of Huang et al. [18].

3.2 Model validation

3.2.1 Schaeffer's model for frictional viscosity

The comparison between experimental measurements and numerical results by Schaeffer's model is shown in **Fig. 2** and **Fig. 3**. The grey lines in **Fig. 2** (a) and (b) marked the magnitude of experimental dynamic angle of repose. In addition, the numerical dynamic angle of repose is defined by the bed surface at the solids volume fraction of 0.3 (approximately half air and half densely packed solid in a cell) [18]. It can be seen that higher specular coefficient results in higher average tangential velocity and higher dynamic angle of repose. With specular coefficient of 0.15, the averaged tangential velocity along the radius at 30° to the vertical is close to the experiment results expect for the velocity near the wall. However, the corresponding dynamic angle of repose is much lower than that of the experiment. With a higher specularity of 0.9, the numerical dynamic angle of repose is close to the experiment results. But there is an evident difference between numerical and experimental velocity. As depicted in **Fig. 3**, the prediction of flow pattern using Schaeffer's model is different with

that in the experiment. The flow pattern in the experiment showed a flat bed surface (without a curve), however, in the numerical results, the bed surface is not flat and evident toe regions occurred. A similar phenomenon was mentioned in Santos' work [9]. Therefore, using Schaeffer's model for frictional viscosity calculation is not suitable for the current work. Since the flow patterns are similar at different rotational speeds, the results of the simulation at 20 rpm and 42 rpm will not be shown in the paper.

3.2.2 Johnson and Jackson model for frictional viscosity

Similarly, the predicted results of the rotating drum at 65 rpm using the Johnson and Jackson model for frictional viscosity are illustrated in **Fig. 4** and **Fig. 5**. With specular coefficient of 0.15, the wall shear stress is too small to lift the solid. With specular coefficient of 0.9, the bed surface is curved, and the dynamic angle of repose is hard to define. The averaged tangential velocity along the radius at 30° to the vertical is close to the experiment results, but a discrepancy occurs in active region which is defined in the paper of the experiment [5]. Additionally, evident toe regions occurred in numerical results like the result of Schaeffer's model as depicted in **Fig. 5**. Therefore, the Johnson and Jackson model for frictional viscosity is not suitable for the current work either.

3.2.3 Proposed model for frictional viscosity

In **Fig. 6**, a good prediction of experimental results was made by the proposed model with appropriate specular coefficients at different rotational speeds, but the tangential velocity near the bed surface is larger than that of measurements. The same feature can also be found in the results of DEM [36], so the deviation may be caused by numerical reasons. It is worth noting that with the increasing of rotational speed, the required specular coefficient decreased. In order to gain insight into current analysis results, a comparison is made with a previous study. In the work of Machado et al [12], the same specular coefficient was used for different rotational speeds. Nevertheless, the averaged of the deviations between numerical and experimental results for solids holdup in the flights were different at different rotational speeds: 9.5% for the rotational speed of 21.3 rpm and 15.4% for the rotational speed of 36.1 rpm. Therefore, in both works, it seems like when only collisional part of the boundary condition was considered, the required specular coefficient changes with rotational speed. However, specular coefficient is defined to be the average fraction of relative tangential

momentum transferred in a particle-boundary collision and its value depends on the large-scale roughness of the surface. For the same particle movement in the same rotating drum, the specular coefficient should be a constant at different rotational speeds. Accordingly, although the prediction using the proposed model with only considering collisional part of boundary condition is good, the boundary condition application is not physically meaningful. A possible explanation is that the specular coefficient used in the calculation is higher than the practical value, so it leads to a proper wall shear stress by coincidence. Thus, an analysis of the wall boundary condition needs to be made.

3.3 Analysis of wall boundary condition

When the frictional contribution in boundary condition is considered, the key parameter is the angle of friction. In the current situation, the angle of friction was hard to determine. Based on the measurement data of similar particles in the work of Huang et al. [18], the angle of friction was assumed in the range of 28.2° - 32° . Considering that the angle of friction is the angle between the surface and the particulate material, the same constant angle should be reasonable for different rotational speeds. Then different combinations of the angle of friction and specular coefficient of the rotating drum at 20 rpm, 42 rpm and 65 rpm were tested. It turned out that when the angle of friction was 30° and the specular coefficient was 0.015, the prediction using the proposed model at three different rotational speeds were good as shown in **Fig. 7**.

The proposed model agreed well with experimental observations by using only collisional part of boundary condition with different specular coefficients or both collisional and frictional part of boundary condition with the same parameters. Based on this phenomenon, it was guessed that the proposed model could be used to predict the experimental results by using only frictional part of boundary condition with different angles of friction. It was very interesting that the guess was verified as shown in **Fig. 8**. Additionally, the velocity field of the rotating drum with all three kinds of boundary conditions are depicted in **Fig. 9**. The flow patterns are very similar. Based on the comparisons of experimental measurements with the numerical results of case 05 to case 07, the proposed model with three different boundary conditions can achieve almost the same prediction. On one hand, the current results supply an explanation for the previous work in which using only collisional part of boundary condition can predict experiment results well. On the other hand, the

frictional and collisional part of boundary condition may have quantitative relationship which needs to be further studied in the future work.

Additionally, case 08 and case 09 were made by using the frictional and collisional part of the boundary condition in case 06, respectively. Experimental and numerical averaged dynamic angle of repose of case 05 to case 09 are shown in **Fig. 10**. When only frictional boundary condition was considered with the same angle of friction of 30° , the dynamic angles of repose are higher than those of considering only collisional boundary condition with the same specular coefficient of 0.015. Therefore, for the solid flow in the current case, the frictional contribution is more than collisional contribution in the wall boundary condition.

4. Conclusions

A Eulerian-Eulerian model coupled to the kinetic theory of granular flow is usually used to study dilute flows. For dense flows, the model can still be used if appropriate frictional viscosity model is taken into account. In the current work, a friction viscosity model based on granular pressure was proposed to study the dense granular flows in a rotating drum. Additionally, the Johnson and Jackson model used for wall boundary condition was discussed.

The simulation results were compared with experimental results in terms of angle of repose and spatial velocity fields. Using the proposed frictional viscosity model, the numerical results agreed well with the experimental measurements by using different boundary conditions. When only the collisional part of boundary condition was used, the appropriate specular coefficients were 0.35, 0.25 and 0.15 for rotating drums at 20 rpm, 42 rpm and 65 rpm. When only frictional part of boundary condition was used, the angles of friction were 35° , 40° and 45° correspondingly. However, when the complete Johnson and Jackson model of boundary condition is used, the specular coefficient and angle of friction are same constants (0.015 and 30°) for different rotational speeds which is more physically meaningful. Moreover, it is found that the friction contributes more to determine the dynamic angle of repose than collision does in the wall boundary condition of the current rotating drum.

Acknowledgements

The authors would like to express their gratitude for the financial support by the CSIRO Mineral Resources and the National Natural Science Foundation of China (Grant No. 51704026). Wenjie Rong (201706080055) would also like to thank the China Scholarship Council (CSC) for a visiting Ph.D. scholarship to support this work.

Journal Pre-proof

References

- [1] M.A. Delele, F. Weigler, G. Franke, J. Mellmann, Studying the solids and fluid flow behavior in rotary drums based on a multiphase CFD model, *Powder Technology* 292 (2016) 260-271.
- [2] Afshin Taghizadeh, Seyed Hassan Hashemabadi, Esmail Yazdani, Soheil Akbari, Numerical analysis of restitution coefficient, rotational speed and particle size effects on the hydrodynamics of particles in a rotating drum, *Granular Matter* (2018) 20-56.
- [3] T. Kawaguchi, MRI measurement of granular flows and fluid-particle flows, *Advanced Powder Technology* 21 (2010) 235-241.
- [4] C.J. Broadbent, J. Bridgwater, D.J. Parker, S.T. Keningley, P. Knight, A phenomenological study of a batch mixer using a positron camera, *Powder Technology* 76 (1993) 317-329.
- [5] D.J. Parker, A.E. Dijkstra, T.W. Martin, J.P.K. Seville, Positron emission particle tracking studies of spherical particle motion in rotating drums, *Chem. Eng. Sci.* 52 (1997) 2011-2022.
- [6] P.A. Cundall, O.D. Strack, A discrete numerical model for granular assemblies, *Geotechnique* 29 (1979) 47-65.
- [7] Zheng, Q. J., and A. B. Yu. "Modelling the granular flow in a rotating drum by the Eulerian finite element method." *Powder technology* 286 (2015): 361-370.
- [8] Mohammad Khalilitehrani, Per J. Abrahamsson, Anders Rasmuson, Modeling dilute and dense granular flows in a high shear granulator, *Powder Technology* 263 (2014) 45-49.
- [9] D.A. Santos, I.J. Petri, C.R. Duarte, M.A.S. Barrozo, Experimental and CFD study of the hydrodynamic behavior in a rotating drum, *Powder Technology* 250 (2013) 52-62.
- [10] D.A. Santos, F.O. Dadalto, R. Scatena, C.R. Duarte, M.A.S. Barrozo, A hydrodynamic analysis of a rotating drum operating in the rolling regime, *Chemical Engineering Research and Design* 94 (2015) 204-212.
- [11] D.A. Santos, C.R. Duarte, M.A.S. Barrozo, Segregation phenomenon in a rotary drum: Experimental study and CFD simulation, *Powder Technology* 294 (2016) 1-10.
- [12] M.V.C. Machado, S.M. Nascimento, C.R. Duarte, M.A.S. Barrozo, Boundary conditions effects on the particle dynamic flow in a rotary drum with a single flight, *Powder Technology* 311 (2017) 341-349.

- [13] Hong Liu, Hongchao Yin, Ming Zhang, Maozhao Xie, Xi Xi, Numerical simulation of particle motion and heat transfer in a rotary kiln, *Powder Technology* 287 (2016) 239-247.
- [14] Y.R. He, H.S. Chen, Y.L. Ding, and B. Lickiss, Solids Motion and Segregation of Binary Mixtures in a Rotating Drum Mixer, *Chemical Engineering Research and Design* 85 (2007) 963-973.
- [15] S.M. Nascimento, D.A. Santos, M.A.S. Barrozo, C.R. Duarte, Solids holdup in flighted rotating drums: An experimental and simulation study, *Powder Technology* 280 (2015) 18-25.
- [16] Wanessa Mendonça Benedito, Claudio Roberto Duarte, Marcos Antonio de Souza Barrozo, Dyrney Araújo dos Santos, An investigation of CFD simulations capability in treating non-spherical particle dynamics in a rotary drum, *Powder Technology* 332 (2018) 171-177.
- [17] Yassine Demagh, Hocine Ben Moussa, Mohammed Lachi, Samira Noui, Lyes Bordja, Surface particle motions in rotating cylinders: Validation and similarity for an industrial scale kiln, *Powder Technology* 224 (2012) 260-272.
- [18] An-Ni Huang, Wei-Chun Kao, Hsiu-Po Kuo, Numerical studies of particle segregation in a rotating drum based on Eulerian continuum approach, *Advanced Powder Technology* 24 (2013) 364-372.
- [19] An-Ni Huang, Hsiu-Po Kuo, CFD simulation of particle segregation in a rotating drum. Part I: Eulerian solid phase kinetic viscosity, *Advanced Powder Technology* 28 (2017) 2094-2101.
- [20] P.C. Johnson, R. Jackson, Frictional-collisional constitutive relations for granular materials, with application to plane shearing, *J. Fluid Mech.* 176 (1987) 67-93.
- [21] Bai, L., Q. J. Zheng, and A. B. Yu. "FEM simulation of particle flow and convective mixing in a cylindrical bladed mixer." *Powder technology* 313 (2017): 175-183.
- [22] Li T, Benyahia S, Revisiting Johnson and Jackson boundary conditions for granular flows. *AIChE J.* 58 (2012) 2058-2068.
- [23] Marcela V. C. Machado, Dyrney A. Santos, Marcos A. S. Barrozo, Claudio R. Duarte, Experimental and Numerical Study of Grinding Media Flow in a Ball Mill, *Chem. Eng. Technol.*, 40 (2017) 1835-1843.
- [24] Xizhong Chen, Junwu Wang, Jinghai Li, Multiscale modeling of rapid granular flow with a hybrid discrete-continuum method, *Powder Technology* 304 (2016) 177-185.

- [25] Afsaneh Soleimani, Simon Schneiderbauer, Stefan Pirker, CFD Study of the Gas particle Flow in a Horizontal Duct: The Impact of the Solids Wall Boundary Conditions *Procedia Engineering*, *Procedia Engineering* 102 (2015) 1026-1037.
- [26] Subrat Kotoky, Amaresh Dalal, Ganesh Natarajan, Effects of specularity and particle-particle restitution coefficients on the hydrodynamic behavior of dispersed gas-particle flows through horizontal channels, *Advanced Powder Technology* 29 (2018) 874-889.
- [27] Yu, L., Lu, J., Zhang, X., Zhang, S., Wang, X., Two fluid model using kinetic theory for modeling of one-step hydrogen production gasifier, *AIChE J.* 54 (2008) 2833-2851.
- [28] Wang, X., Yu, L., Wang, J., Numerical Simulation of Effect of Internals on Slugging Fluidization and Analysis of Nonuniformity Index, *International Journal of Chemical Reactor Engineering* 10 (2012) Article A77.
- [29] Peng Li, Xuhui Zhang, Xiaobing Lu, Numerical simulation on solid-liquid two-phase flow in cross fractures, *Chemical Engineering Science* 181 (2018) 1-18.
- [30] Afsaneh Soleimani, Simon Schneiderbauer, Stefan Pirker, Numerical study of the gas-particle flow in a conveying line: accounting for wall-friction and wall-roughness, 10th International Conference on CFD in Oil & Gas, Metallurgical and Process Industries SINTEF, Trondheim, Norway 17-19 June 2014.
- [31] Liang Yu, Jingwei Ma, Craig Frear, Quanbao Zhao, Robert Dillon, Xiujin Li, Shulin Chen, Multiphase modeling of settling and suspension in anaerobic digester, *Applied Energy* 111 (2013) 28-39.
- [32] Jan Hendrik Cloete, Schalk Cloete, Stefan Radl, Shahriar Amini, Evaluation of wall friction models for riser flow, *Powder Technology* 303 (2016) 156-167.
- [33] Hui K, Haff PK, Ungar JE, Boundary conditions for high-shear grain flows. *J Fluid Mech.* 145 (1984) 223-233.
- [34] Y. Zhao, T. Ding, L. Zhu, Y. Zhong, A specularity coefficient model and its application to dense particulate flow simulations, *Ind. Eng. Chem. Res.* 55 (2016) 1439-1448.
- [35] Louge, M. Y., Computer-Simulations of Rapid Granular Flows of Spheres Interacting with a Flat, Frictional Boundary, *Phys. Fluids* 6 (1994) 2253-2269.

- [36] R.Y. Yang, R.P. Zou, A.B. Yu, Microdynamic analysis of particle flow in a horizontal rotating drum, *Powder Technology* 130 (2003) 138-146.
- [37] R.Y. Yang, A.B. Yu, L. McElroy, J. Bao, Numerical simulation of particle dynamics in different flow regimes in a rotating drum, *Powder Technology* 188 (2008) 170-177.
- [38] ANSYS, ANSYS FLUENT 19 Theory Guide, ANSYS Inc., Canonsburg, PA, USA, 2018.
- [39] D. Gidaspow, R. Bezburuah, and J. Ding, Hydrodynamics of Circulating Fluidized Beds, Kinetic Theory Approach, In *Fluidization VII, Proceedings of the 7th Engineering Foundation Conference on Fluidization*. (1992) 75-82.
- [40] C. K. K. Lun, S. B. Savage, D. J. Jeffrey, and N. Chepuruiy, Kinetic Theories for Granular Flow: Inelastic Particles in Couette Flow and Slightly Inelastic Particles in a General Flow Field, *J. Fluid Mech.* 140 (1984) 223-256.
- [41] J. Ding and D. Gidaspow, A Bubbling Fluidization Model Using Kinetic Theory of Granular Flow, *AIChE J.* 36 (1990) 523-538.
- [42] C. K. K. Lun, S. B. Savage, D. J. Jeffrey, and N. Chepuruiy. "Kinetic Theories for Granular Flow: Inelastic Particles in Couette Flow and Slightly Inelastic Particles in a General Flow Field". *J. Fluid Mech.* 140 (1984) 223-256.
- [43] S. Ogawa, A. Umemura, N. Oshima, On the Equation of Fully Fluidized Granular Materials, *J. Appl. Math. Phys.* 31 (1980) 483-493.
- [44] B.G.M. Van Wachem, J.C. Schouten, C.M. van den Bleek, R. Krishna, J.L. Sinclair, Comparative analysis of CFD models of dense gas-solid system, *AIChE Journal* 47 (5) (2001) 1035-1051.
- [45] Coulomb, C. A., *Essai sur Une Application des Règles de Maximis et Minimis à Quelques Problèmes de Statique, Relatifs à l'architecture*, Acad. R. Sci. *Mém. Math, Phys. Divers. Sauvants*, 7 (1776) 343-382.
- [46] D. G. Schaeffer, Instability in the Evolution Equations Describing Incompressible Granular Flow, *J. Diff. Eq.* 66 (1987) 19-50.
- [47] P. C. Johnson, P. Nott, R. Jackson, Frictional-collisional equations of motion for particulate flows and their application to chutes, *J. Fluid Mech.* 210 (1990) 501-535.

- [48] R. Ocone, S. Sundaresan, R. Jackson, Gas-Particle Flow in a Duct of Arbitrary Inclination with Particle-Particle Interactions, *AIChE Journal* 39 (1993) 1261-1271.

Journal Pre-proof

Tables

Table 1. Parameters in the simulation.

Parameters	Value
Drum diameter (m)	0.1
Drum fill level	35%
Drum rotational speeds (rpm)	20/42/65
Particle diameter (m)	0.003
Particle density (kg/m^3)	2500
Particle restitution coefficient	0.9

Table 2. Different model configurations.

Case	Frictional viscosity model	Specularity coefficient (for 20/42/65rpm)	Angle of friction (for 20/42/65rpm)
01	Schaeffer's model	0.15/0.15/0.15	-
02	Schaeffer's model	0.9/0.9/0.9	-
03	Johnson and Jackson model	0.15/0.15/0.15	-
04	Johnson and Jackson model	0.9/0.9/0.9	-
05	Proposed model	0.35/0.25/0.15	-
06	Proposed model	0.015/0.015/0.015	30°/30°/30°
07	Proposed model	-	35°/40°/45°
08	Proposed model	-	30°/30°/30°
09	Proposed model	0.015/0.015/0.015	-

Fig.2. Comparison of experimental results with numerical results. (a) dynamic angle of repose of case 01, (b) dynamic angle of repose of case 02, (c) averaged tangential velocity along the radius at 30° to the vertical.

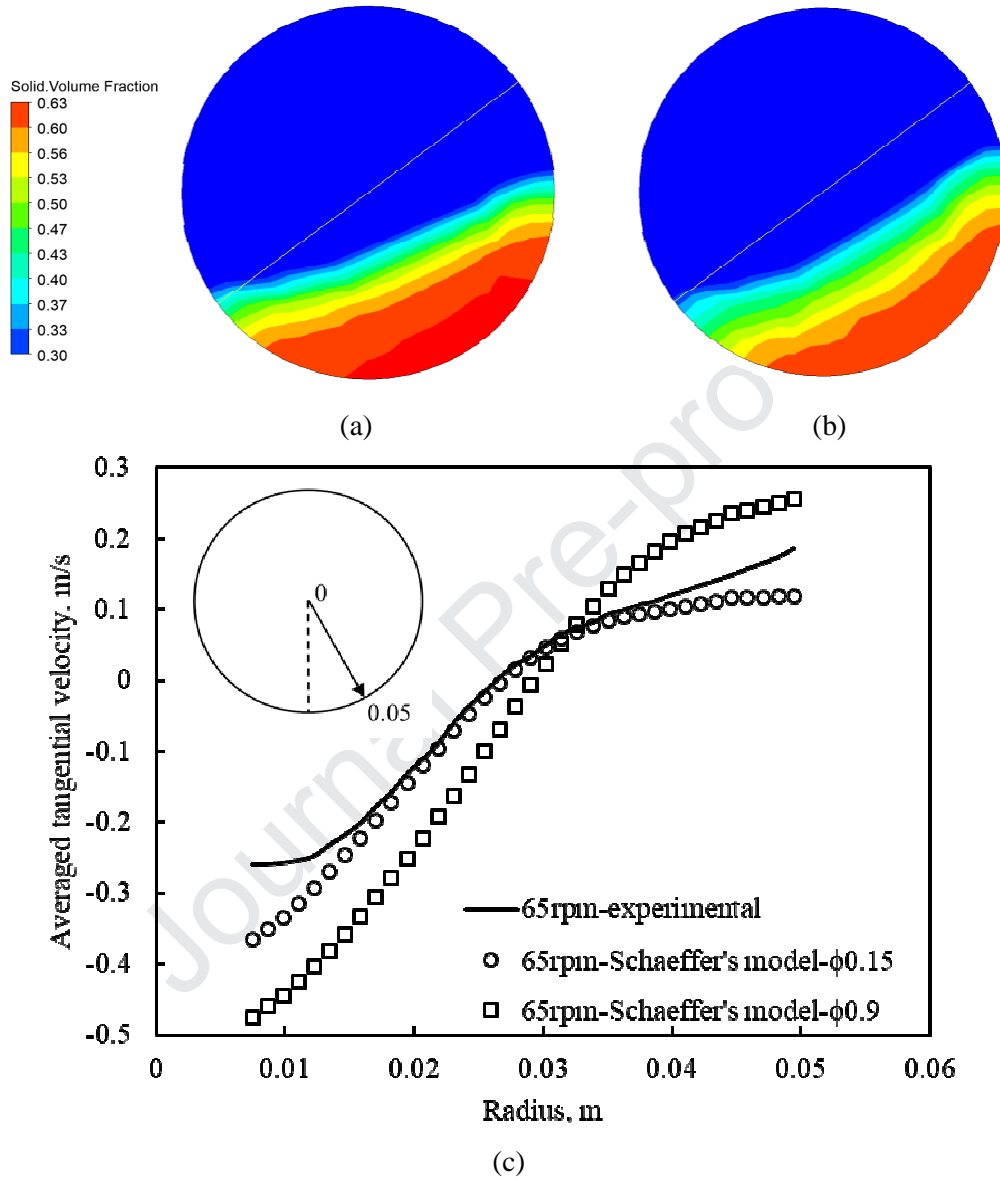


Fig.3. Experimental (a) and numerical flow patterns of case 01(b) and case 02 (c) at the rotational speeds of 65 rpm.

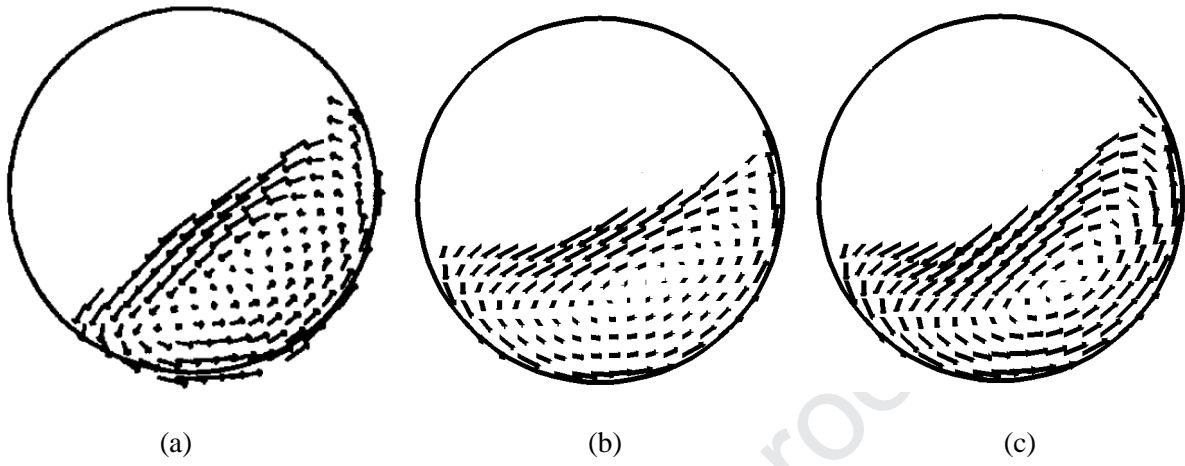


Fig.4. Comparison of experimental results with numerical results. (a) dynamic angle of repose of case 03, (b) dynamic angle of repose of case 04, (c) averaged tangential velocity along the radius at 30° to the vertical.

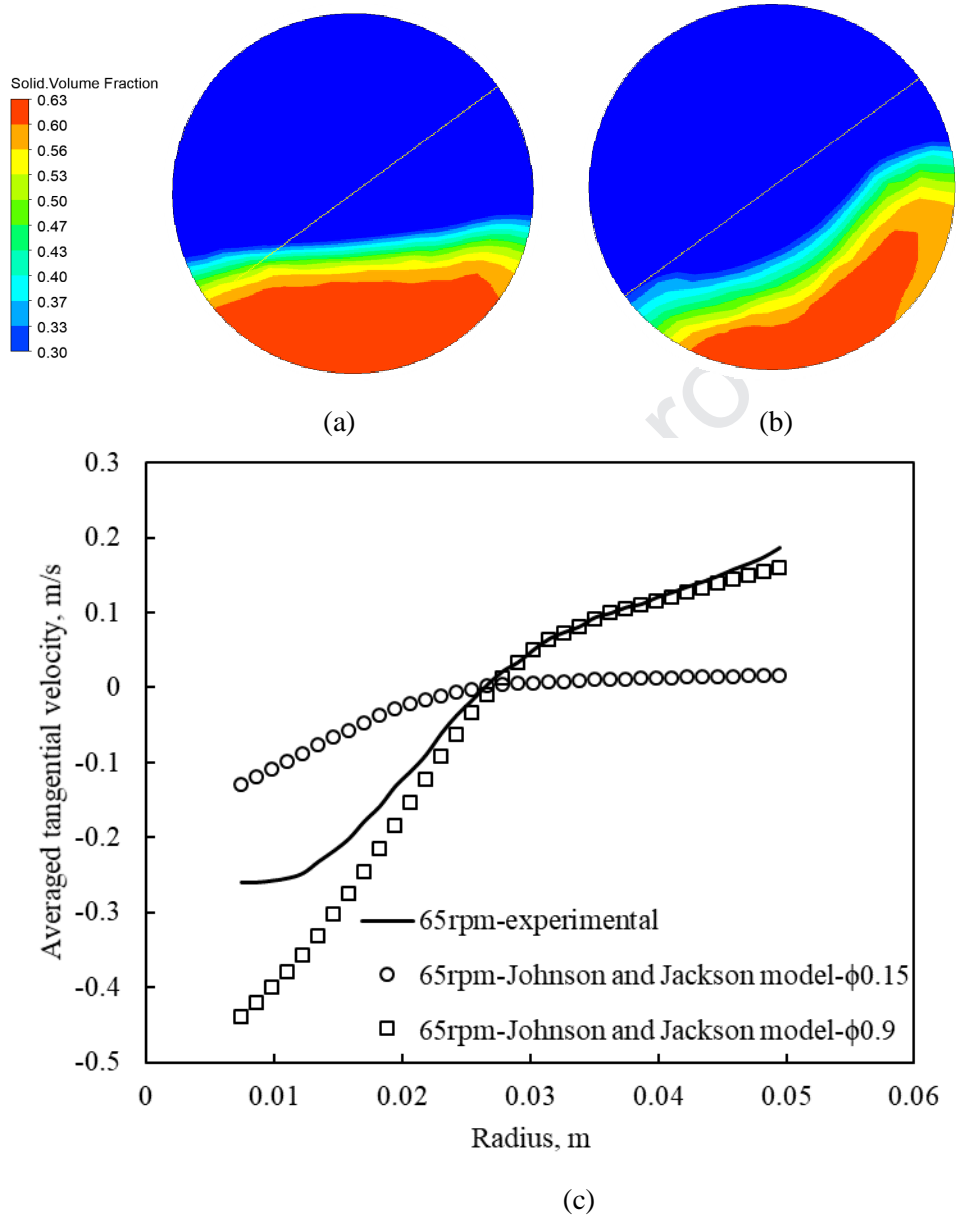


Fig.5. Experimental (a) and numerical flow patterns of case 03 (b) and case 04 (c) at the rotational speeds of 65 rpm.

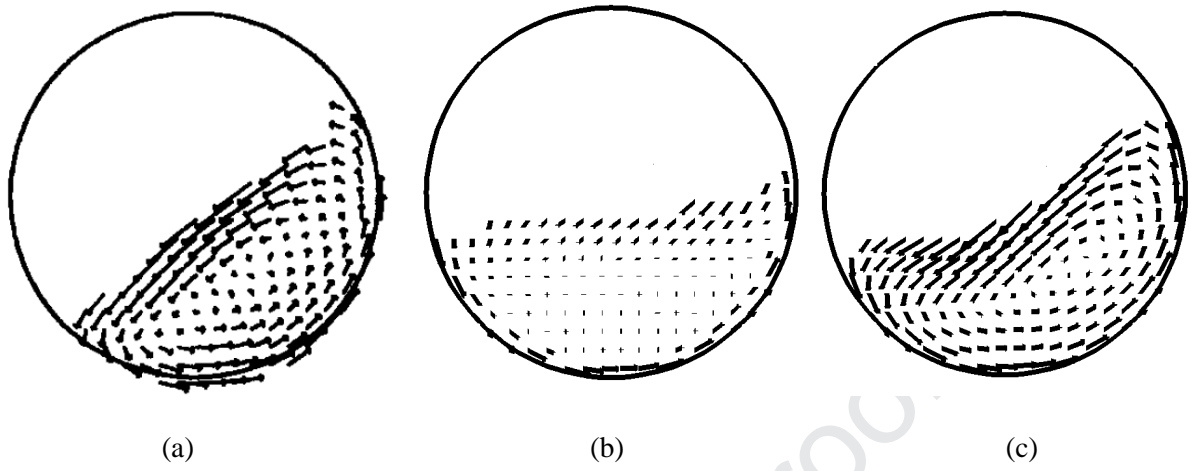
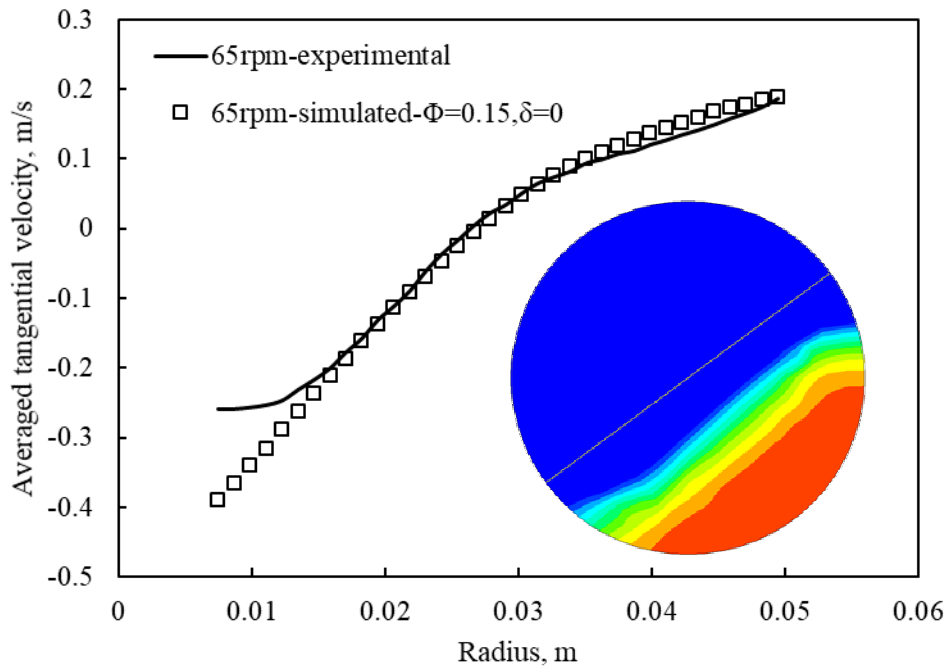
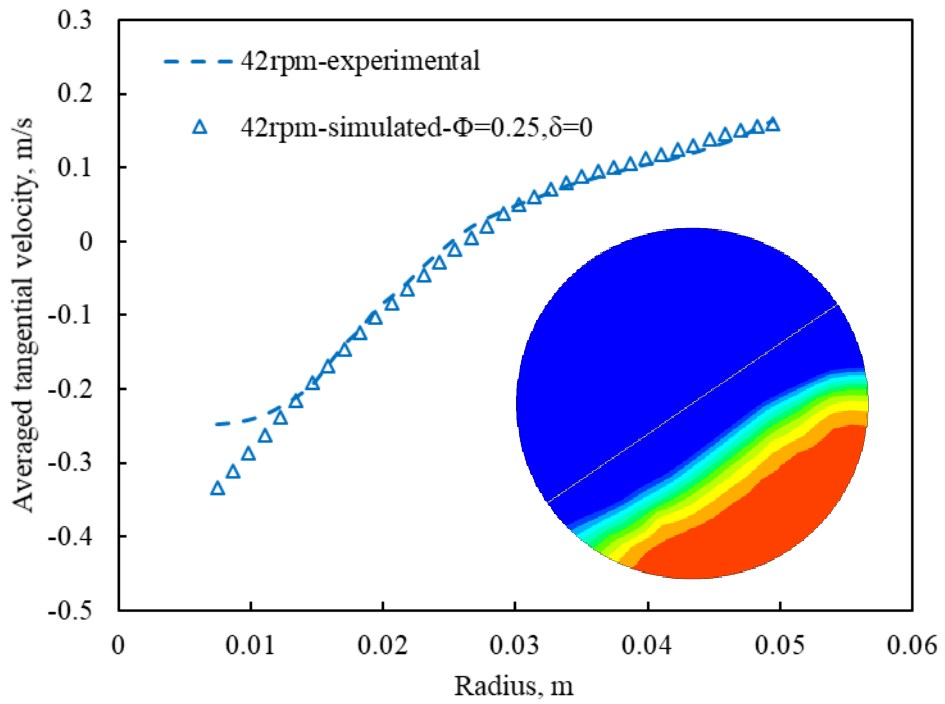


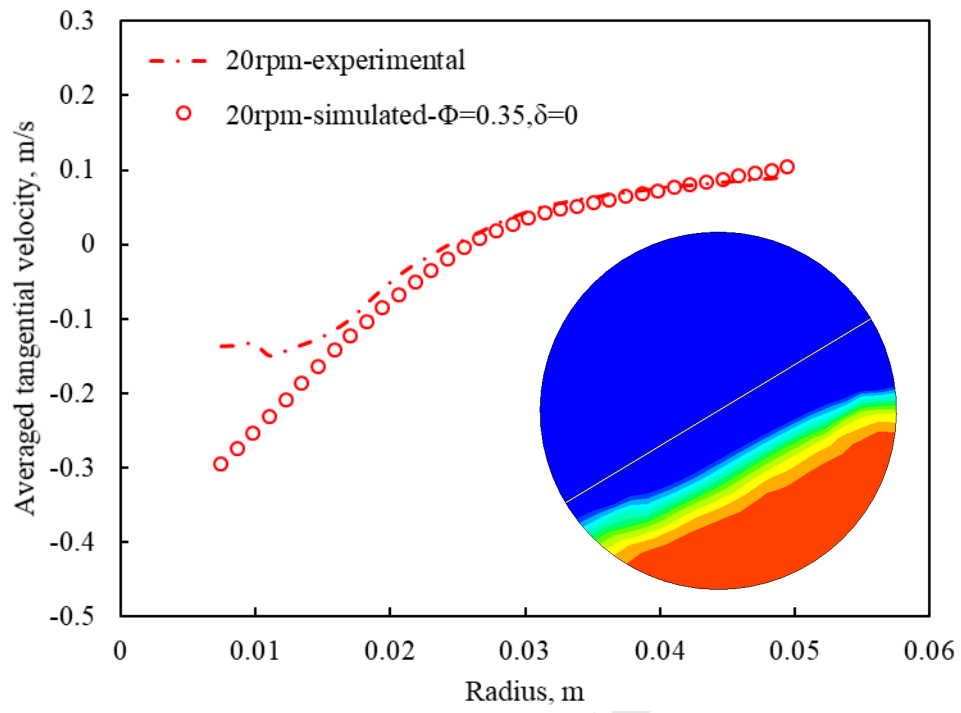
Fig.6. Comparison of experimental results with numerical results of case 05.



(a)

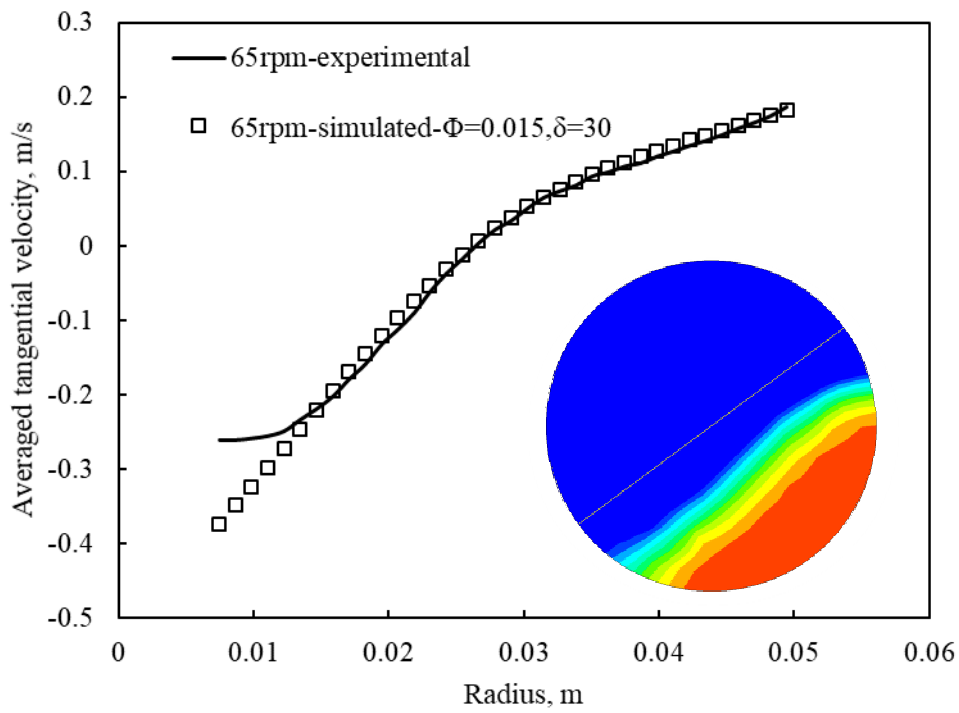


(b)

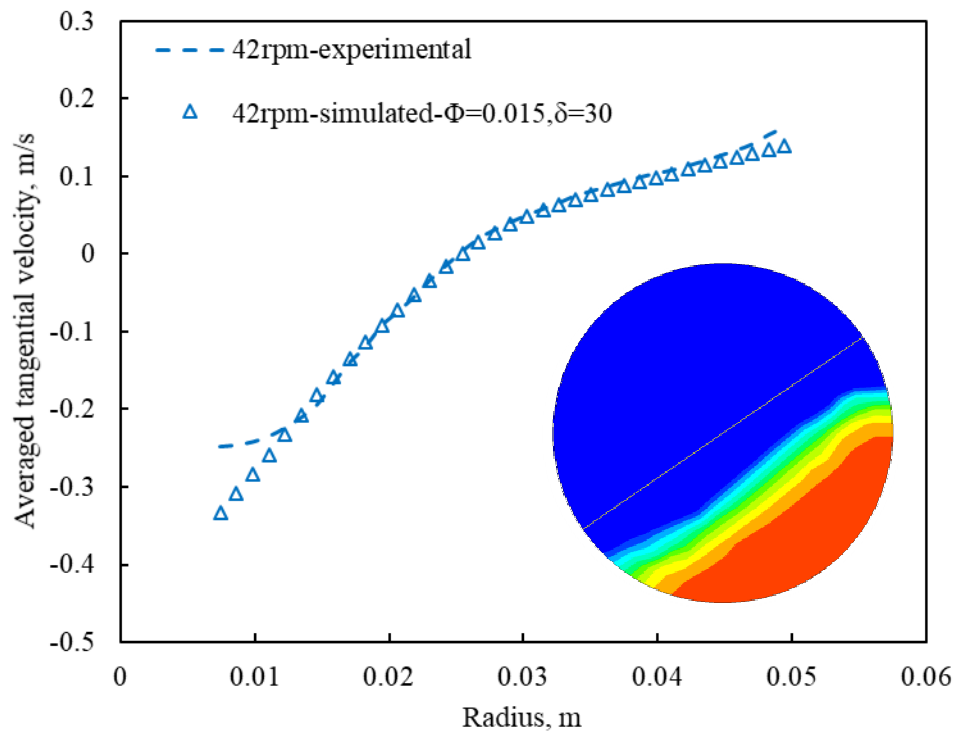


(c)

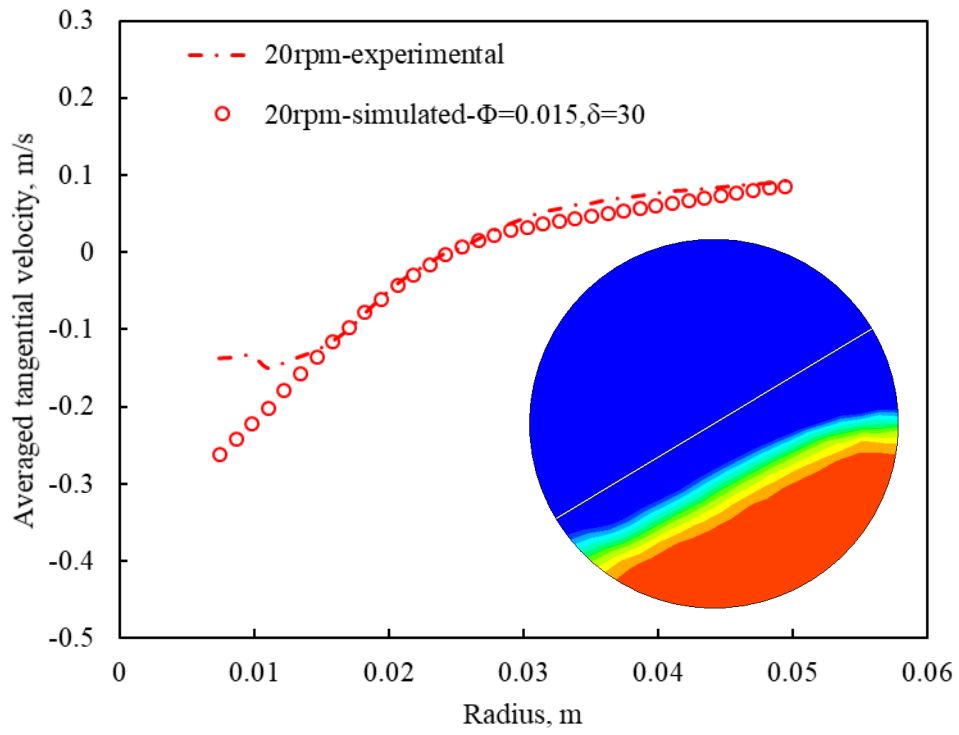
Fig.7. Comparison of experimental results with numerical results of case 06.



(a)

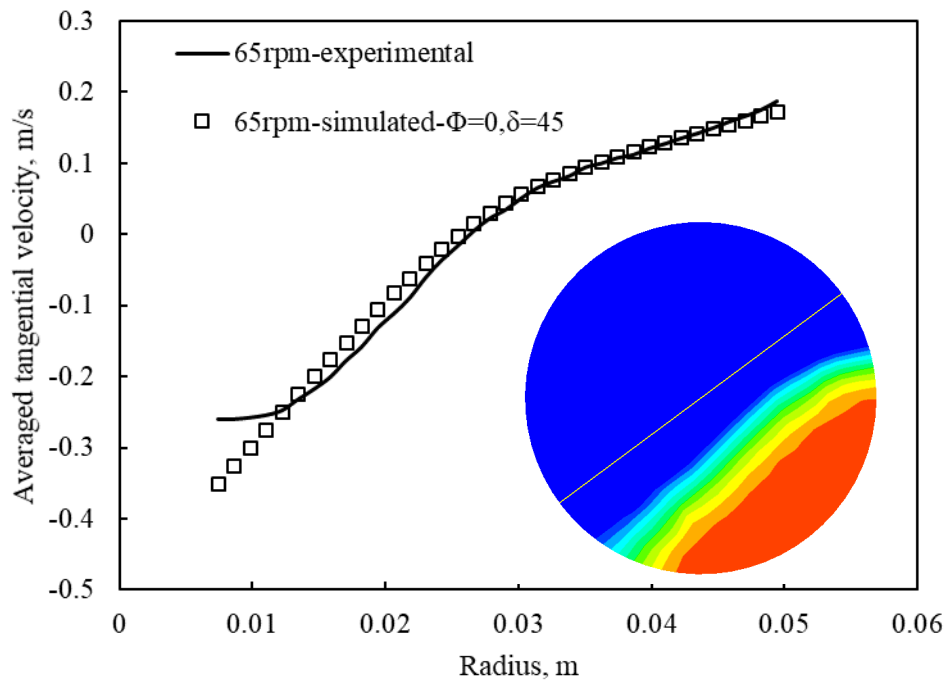


(b)

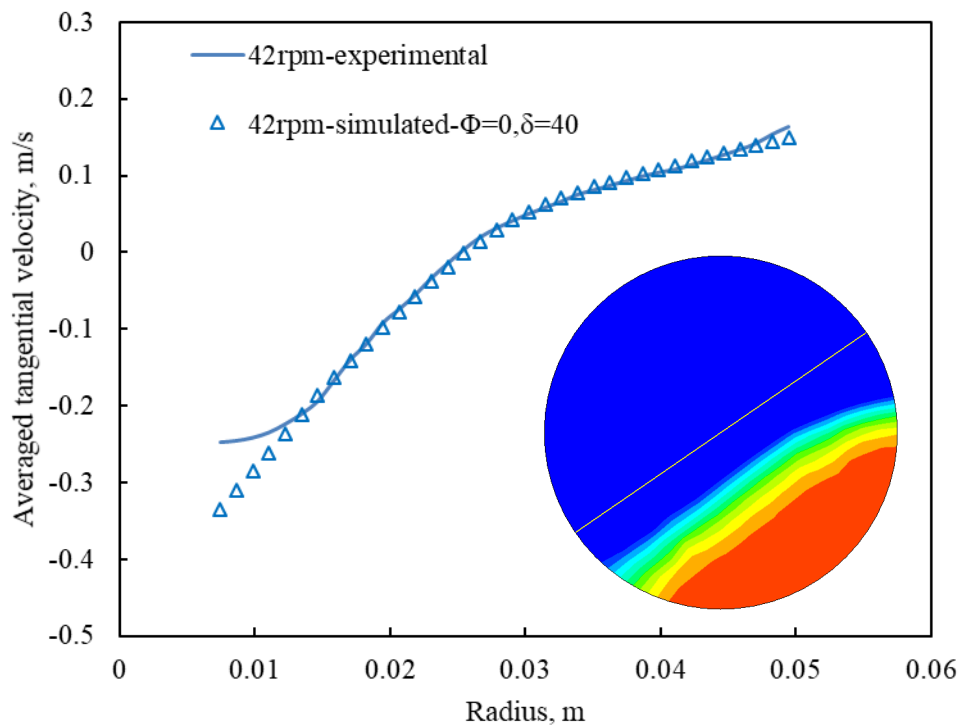


(c)

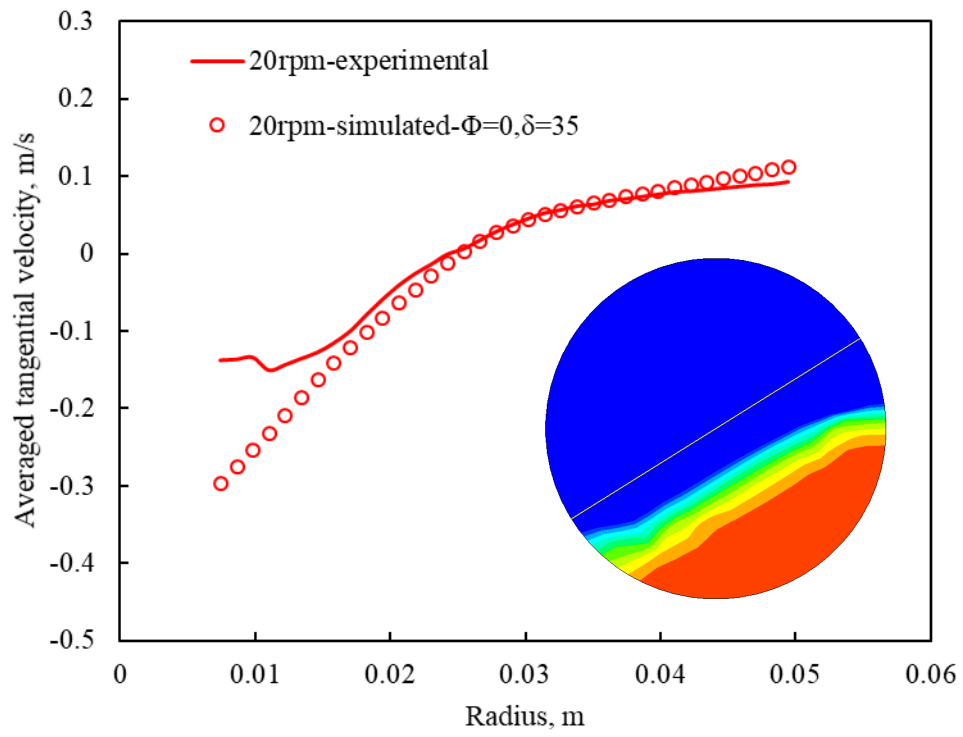
Fig.8. Comparison of experimental results with numerical results of case 07.



(a)



(b)



(c)

Fig.9. Experimental and numerical flow patterns of case 05, case 06 and case 07 at rotational speeds of 20 rpm, 42 rpm and 65 rpm from left to right.

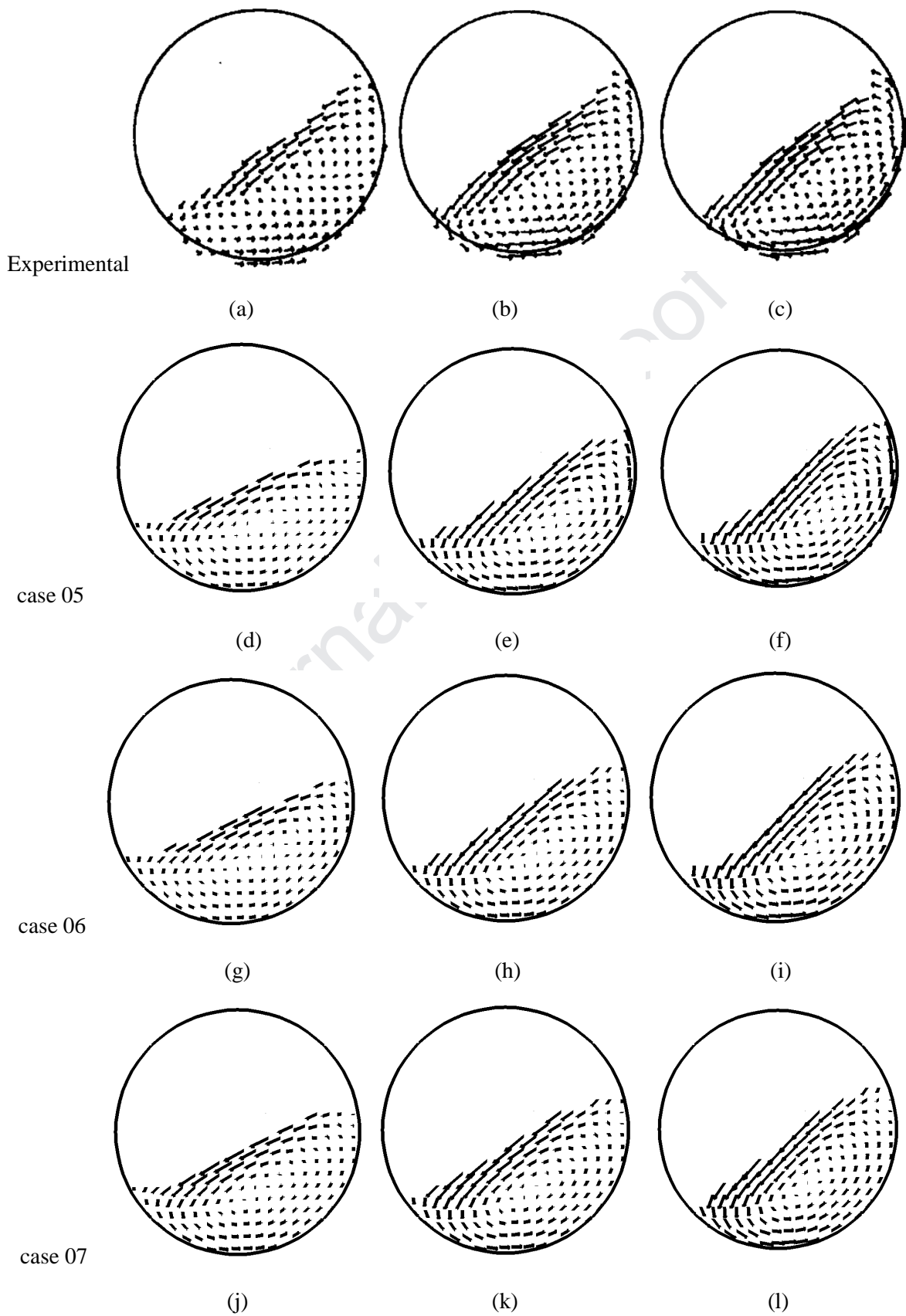
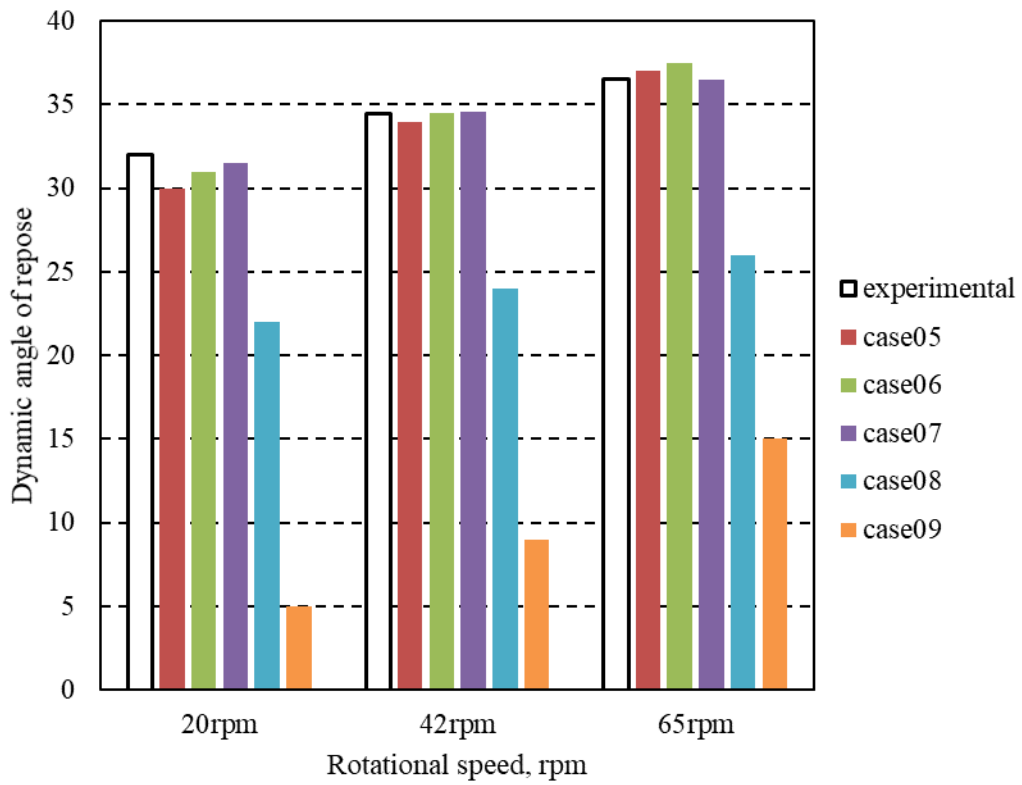


Fig.10. Experimental and numerical averaged dynamic angle of repose.



Highlights

1. A frictional viscosity model based on granular pressure was proposed.
2. Johnson and Jackson model for boundary condition was analyzed.
3. Friction has greater impact on dynamic angle of repose than collision in the wall.

Journal Pre-proof